On plankton distributions and biophysical interactions in diverse coastal and limnological environments

Nayak, Aditya, McFarland, Malcolm , Twardowski, Michael, Sullivan, James

Aditya R. Nayak, Malcolm N. McFarland, Michael S. Twardowski, James M. Sullivan, "On plankton distributions and biophysical interactions in diverse coastal and limnological environments," Proc. SPIE 10631, Ocean Sensing and Monitoring X, 106310P (25 May 2018); doi: 10.1117/12.2309798

SPIE.

Event: SPIE Defense + Security, 2018, Orlando, Florida, United States

On plankton distributions and biophysical interactions in diverse coastal and limnological environments

Aditya R. Nayak[a], Malcolm N. McFarland[a], Michael S. Twardowski[a], and James M. Sullivan[a]

[a]Harbor Branch Oceanographic Institute at Florida Atlantic University, 5600 US 1 North, Fort Pierce, Florida 34952, USA

ABSTRACT

Digital holography provides a unique perspective towards studying aquatic particles/organisms. The ability to sample particles in undisturbed conditions, coupled with the ability to generate 3-D spatial distributions is currently unmatched by any other technique. To leverage these advantages, field experiments with the goal of characterizing aquatic particle properties *in situ*, were conducted using a submersible holographic imaging system. Diverse aquatic environments were sampled over 3 separate deployments between 2014 and 2017. The areas included: (a) The Gulf of Mexico (GoM), in the vicinity of the Mississippi river plume; (b) Lake Erie; and (c) East Sound in the US Pacific Northwest. A database of more than two million different types of particles in the 10-10000 m size range, was created after processing $>$ 100,000 holograms. Particle size distributions (PSDs) exhibited a Junge-type distribution when characterized by size grouping into logarithmically spaced bins. Particles/plankton were also classified into different groups (e.g. diatoms, copepods). Results presented will be broadly grouped into two parts: (a) PSDs at different depths within the water column during the occurrence of a *Microcystis* bloom at Lake Erie and individual cell counts within these colonies; and (b) Vertical structure of plankton in East Sound, specifically the presence of diatom thin layers. Finally, the rich diversity in species composition in the GoM and successful data collection towards creating a training set to implement automated classification routines will be briefly discussed.

Keywords: Digital holography, phytoplankton, particle size distributions, marine optics

1. INTRODUCTION

The oceanic waters are densely populated by billions of vastly diverse particles.[1] For example, the particle field in a small water sample could potentially comprise both living and non-living matter, including sediment particles, phytoplankton, zooplankton, and/or marine snow.These particles occur in a range of sizes and shapes and inhabit all the world's oceans, from the frigid Arctic/Antarctic regions to the tropical waters in low-latitudinal areas. Particles could range from picoplankton, which could be as small as 0.2 μm in diameter, to colonial diatoms, which can form colonies several cm in length. Due to their ubiquitous nature, particles play a major role in several important areas, spanning the spectrum of ocean sciences. For example, with increasingly warmer waters, and enhanced carbon absorption in the upper oceans, particles act as pathways to sequester this carbon to the sea-floor.[2] In coastal regions, quantification of sediment resuspension and transport is critical to modelers and engineers addressing erosion problems.[3] Particles can also be used as tracers to study the small-scale flow structure and turbulence in the ocean.[4,5] Particles are not homogeneously distributed throughout the water column; understanding propagation of light through diverse particle fields in the water column is relevant to remote sensing and marine ecology. For example, it has been recently shown that preferential particle orientation can modify the backscattering of light in the oceans.[6,7]Thus, it is important to characterize particle/plankton distributions and interactions in the world's oceans.

Particle populations are quantified by either direct or indirect methods. Indirectly, particle properties are inferred from inverse methods related to either acoustic or optical propagation through the water column.[8,9] Inherently, this method is rife with assumptions about the particle field *a priori*, e.g., all particles are assumed to

Further author information: (Send correspondence to A.R.N.)
A.R.N.: E-mail: anayak@fau.edu, Telephone: 1 772 242 2427

Ocean Sensing and Monitoring X, edited by Weilin (Will) Hou, Robert A. Arnone, Proc. of SPIE
Vol. 10631, 106310P · © 2018 SPIE · CCC code: 0277-786X/18/$18 · doi: 10.1117/12.2309798

be spheres, which is more often than not, an unrealistic depiction. Direct methods, wherein particle counts are obtained directly, can further be broadly grouped into (i) shipboard analysis of discrete water samples and (ii) *in situ* methods. Water samples are collected via Niskin bottles and/or net tows and analyzed through standard microscopy, or cytometry.[9] However, these methods of collection and analysis can lead to particle breakage, either during sampling or while passing through a flow chamber, leading to bias in the data towards smaller particle sizes. The most accurate statistics are thus provided by *in situ* imaging methods that allow for remote sampling of relatively large sample volumes, while slowly profiling the entire depth of the water column.Significant advances since the turn of the millennium have led to enhanced capabilities in digital imaging, data storage methods/space and reduction in computational costs. This has enabled high frequency *in situ* sampling of particle fields and faster post-processing, thus leading to increased research in this area of focus.[10]

Digital holography is one such imaging technique, which has been increasingly used in recent years in studies of particle-flow dynamics and biophysical interactions in natural environments.[7,11,12] Holography is a non-intrusive technique which fully resolves particle distributions within a 3-D sampling volume. Briefly, the technique involves using a coherent light source (e.g., laser) to illuminate the region of interest to record the diffraction patterns caused by the interference of light scattered by the particles and the undisturbed source beam.[13] Numerical reconstruction techniques can then be used to reconstruct 2-D planes at different lateral distances within the sample volume.[14] Thus, each hologram has the ability to provide the spatial 3-D distributions of all particles within the sampling volume. A time series of this data can then be used to analyze spatial and temporal variations in particle fields, thus opening up an array of questions that could be potentially addressed.

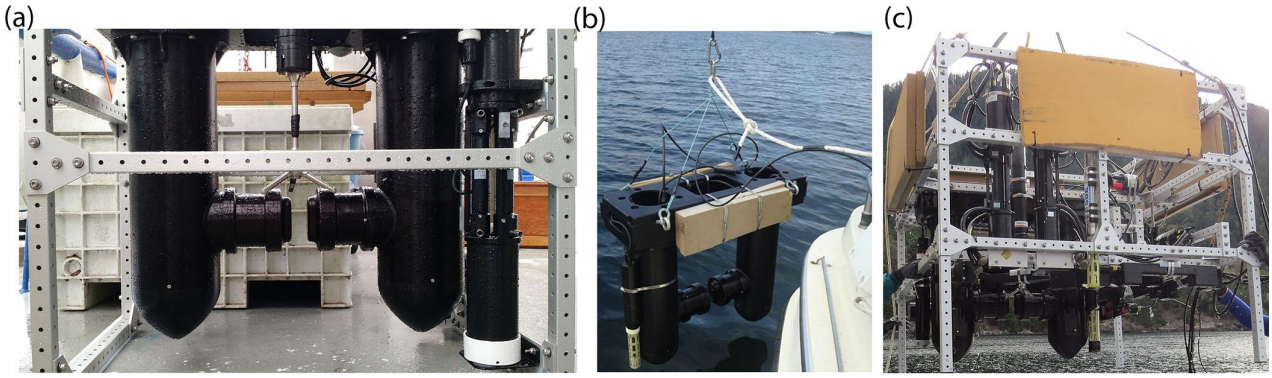

Figure 1. The HOLOCAM during various cruises/configurations: (a) A close-up of the HOLOCAM package during the deployment in the Gulf of Mexico in May 2017. The typical location of the ADV with respect to the HOLOCAM can also be seen here; (b) The HOLOCAM being deployed standalone in Lake Erie (Aug 2014); and (c) HOLOCAM with a much larger instrumentation suite containing various optical/acoustic sensors at East Sound in the Pacific Northwest (September 2015)

This paper reports on the deployment of a submersible holographic imaging system (HOLOCAM) to characterize particle fields in diverse aquatic environments, including lakes, coastal oceans and fjords. The HOLOCAM has been deployed in various configurations including as part of a comprehensive optical instrumentation suite, along with acoustic instrumentation to characterize local small-scale turbulence, or standalone. The field experiments will be described in Section 2 with a brief overview of the methodology, while sample results from each of the three different field sites will be detailed in Section 3. We will conclude with a brief summary and discussion of the results and current/future work in Section 4.

2. MATERIALS AND METHODS

2.1 Submersible Holographic Imaging System

The HOLOCAM is a dual-resolution imaging system with two separate sample volumes, suitable for deployment at depths up to 300 m. A 660 nm Nd-YAG laser acts as the coherent illumination source for the sample volume, with a camera recording the resulting holograms. A laser at this particular wavelength is chosen because red

light attenuates fastest underwater. Secondly, most aquatic organisms are insensitive to light in this region of the visible spectrum. The two sample volumes have different resolutions: the high resolution data is recorded at 0.34 μm/pixel (field of view, FOV = 0.83 x 0.77 mm), while the low resolution data is acquired at 4.29 - 4.59 μm/pixel (FOV = 8.79 x 8.79 mm - 9.4 x 9.4 mm), during different deployments (the corresponding camera is spatially shifted by a small distance between each deployment). Further details regarding the HOLOCAM specifications as well as how the streamlined design helped minimize flow disturbance in the sampling volume are provided in Nayak et al.[7] Only data from the low resolution sample volume is discussed here, as the focus is on large particles.

2.2 Field Measurements

The HOLOCAM was deployed either standalone or as part of a larger instrumentation suite, at three different locations representing diverse aquatic environments, over the span of 4 years. Briefly, the locations included: (a) East Sound, a fjord in the Pacific Northwest; (b) Lake Erie in Michigan; and (c) the Gulf of Mexico, in the vicinity of the Mississippi river plume. More information on the specific locations and mode of deployment is provided in the relevant sections. In all cases, the HOLOCAM recorded data during both descent and ascent.The system was hand deployed at a rate of 4-5 cm/s, which enabled slow profiling of the entire water column. During ascent, the sample volume was in the wake of the system, thus the flow was well and truly mixed, thus enabling comparisons of the particle fields in both disturbed/undisturbed environments. Nayak et al.[7] provide further details of deployment procedures during a typical HOLOCAM profile.

2.3 Data Processing Techniques

Broadly, the processing involved to derive the particle distribution from a single raw hologram can be segregated into three steps: (a) subtraction of the mean image from a time series of holograms, which eliminates background intensity variations; (b) hologram reconstruction, which involves using numerically implementing the Fresnel diffraction formula,[14] thus yielding in-focus particles at different planes within the 4 cm sample volume; and (c) generating a composite image, where all the in-focus particles are collapsed onto one plane to facilitate post-processing. Various image processing and segmentation routines are then applied to the composite image to isolate each individual particle, and create a database of several particle statistics, including but not limited to, major axis length (MAL), aspect ratio (AR), orientation etc., for each hologram, and by extension, for the entire profile. An exhaustive description on these methods has already been provided elsewhere.[7] In the rest of the manuscript, particle sizes are quantified using either the major axis length (MAL, which corresponds to the longest particle dimension), and/or equivalent size diameter (D). The equivalent size diameter is defined as $D = \sqrt{4A/\pi}$, where A is the area of the particle.

3. RESULTS

This section will be further sub-divided into three parts based on the different field locations. While only a few profiles for each case are discussed here, the datasets chosen are representative of most of the datasets collected at that particular location. Specifically, particle size distributions, vertical distributions of plankton, and interesting phenomenon related to plankton 'patchiness' such as 'thin layers' and harmful algal blooms are discussed.

3.1 East Sound, Washington

3.1.1 Site description

East Sound is a fjord in Washington state in the Pacific Northwest. The general location has been well-studied, with several efforts to study biophysical interactions in the last few decades.[12,15] The HOLOCAM was deployed as part of a combined optical and acoustic instrumentation suite for two weeks in September 2015. Further details on the other instruments and the package itself can be found elsewhere.[16] For the purposes of this study, primarily the HOLOCAM data from two depth profiles (referred to as ES1 and ES2 henceforth) which were recorded in quick succession to each other will be used to present particle characteristics. 2850 and 1467 holograms were analyzed respectively at each of the stations, ES1 and ES2.

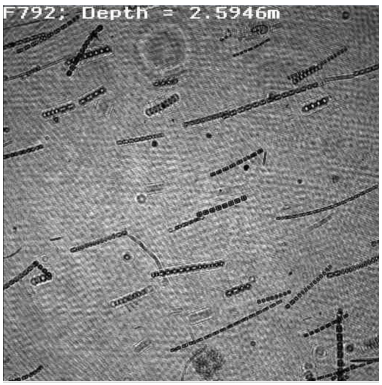

Figure 2. Video 1: A movie made of 190 holograms acquired while the HOLOCAM slowly profiled through a 'thin layer' during one of the depth casts at East Sound. A clear increase in particle abundance is seen around 2.7 m. http://dx.doi.org/10.1117/12.2309798.1

3.1.2 'Thin layer' formation

Video 1 shows the raw feed from the HOLOCAM during one descent. The movie is composed of 190 holograms, with each frame depth-labeled to indicate the depth during the profile.It should be noted that these are *unprocessed* holograms; hence a majority of the particles are not in focus. Halfway through the movie, a sudden increase in particle abundance occurs, lasting several seconds. Further below, the particle field drops back to the background level. This happens as the HOLOCAM is slowly transecting a 'thin layer' - a narrow, temporally coherent patch of phytoplankton, which is strongly correlated to the local physical properties of the water column. Oftentimes, this is seen to coincide with the presence of a strong, stably stratified zone (pycnocline).[17]In this case, the 'thin layer' is caused by the presence of long aspect ratio particles which are dominated by *Ditylum brightwelli*, a species of colonial diatom. To further evaluate the 'thin layer' composition, all *Ditylum sp.* have been isolated from the entire particle field. Following this, the data has been binned into 20 cm depth bins, i.e., all diatoms in holograms within a particular depth bin are counted. The process is repeated for each depth bin through the water column, generating a vertical profile of diatom counts.The concentrations (mL^{-1}) are then calculated by dividing the count by the sample volume of each hologram times the number of holograms per depth bin. Figure 3a shows the chlorophyll-a (chl-a) depth profile for ES1. A clear spike in the chl-a signature is seen

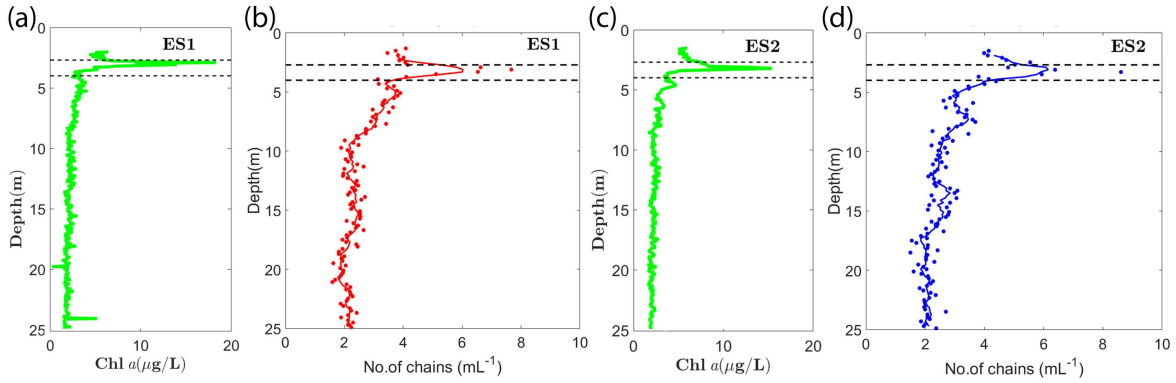

Figure 3. (a) Chl-a profile for station ES1; (b) Variations in diatom chain distribution of *Ditylum sp.* with depth for ES1; (c) Chl-a profile for station ES2; and (d) Depth variations in diatom chain distribution for ES2. Bold dashed lines represent extent of the pycnocline in both cases.Note the chl-a peak within the pycnocline, constituting the 'thin layer'. The 'thin layer' was primarily driven by *Ditylum sp.*, as evidenced by peak in the diatom concentrations at same spatial location.

between 2.7-4 m (the rough extent of the thermocline, indicated by the dotted line). The diatom concentration

with depth for the same station (ES1) is shown in Figure 3b. The solid line is a 5 point running average of the binned data. A distinct correlation between the chl-a peak and the enhanced diatom concentrations can be seen, implying that the 'thin layer' of diatoms is what is primarily driving the increased chl-a (and not smaller particles which might not be resolved by our data). Similar trends are seen in chl-a and diatom chain concentrations for ES2 (Fig 3c and 3d). A further comparison of diatom concentrations as a function of the chain lengths (MAL), within and outside the 'thin layer' is also carried out. Here, only diatom chains 375 μm and longer are considered for analysis and the data is binned into 250 μm size bins. For example, all diatoms with chain lengths ranging from 375-625 μm are binned in the 500 μm bin, while chain lengths between 625-875 μm are grouped under the 750 μm bin, and so on. Figure 4a and 4b show the 'relative frequency of occurrence', which is essentially the ratio of the diatom chain concentrations (mL^{-1}) within the layer to concentrations outside the layer. For example, in Figure 4a, the diatom chains with lengths 500 μm are present at concentrations 1.5 times higher within the layer than outside. Similarly, diatom chains with lengths of 2500 μm are nearly 4.5 times higher in concentration within the layer. The trends for both runs (Figure 4a and 4b) show that most of the longer chains are present within the 'thin layer', with the relative increase peaking around the 2500 μm mark for both ES1 and ES2. This could potentially be related to higher availability of light at the surface, and/or other favorable conditions within the layer, leading to enhanced growth rates and lengths.

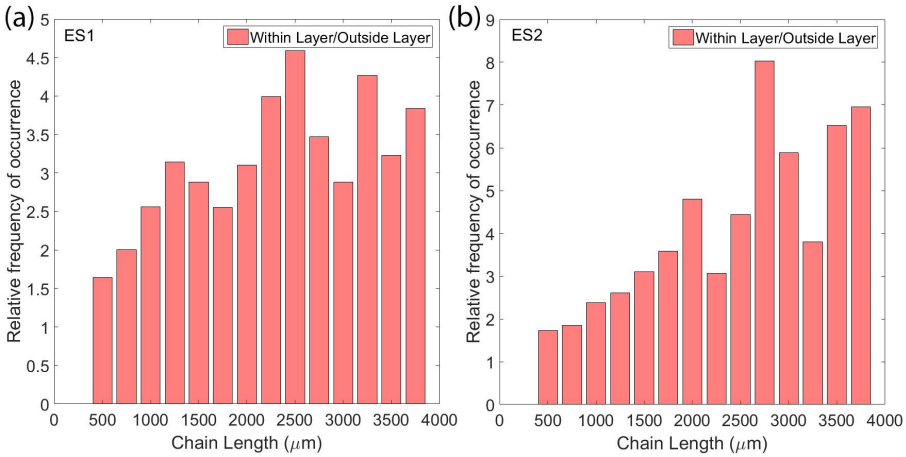

Figure 4. (a) The ratio of diatom chains within and outside the 'thin layer' as a function of chain lengths (MAL) for ES1; (b) The ratio of diatom chains within and outside the 'thin layer' as a function of chain lengths(MAL) for ES2

3.1.3 Particle size distributions

As the two datasets, ES1 and ES2, exhibit similar particle characteristics, we choose to show the particle size distributions(PSDs) for only one run (ES1) here. To better understand the nature of the particle fields at the given location, this analysis is not limited to only the diatom chains, but all recorded particles. Typically, the power law (or Junge) distribution is used to represent oceanic PSDs.[18,19] The exponent -γ represents the slope of the Junge distribution, where the steeper the slope (higher -γ), the higher the concentration of smaller particles. Flatter slopes imply larger particles are present in relatively high numbers. The data is binned into logarithmically spaced size bins, with the differential particle concentrations represented with units L^{-1} μm^{-1}. For ES1, the PSDs are analyzed in 3 m depth bins throughout the entire water column (Figures 5a-5h). There is a distinct bump between D=275-300 μm at 2.5 m (Fig 5a). This depth bin corresponds to the spatial location of the 'thin layer', where an enhanced number of long aspect ratio particles in this size range lead to this bump at these particular range of D values. In Figures 5b-5h, there are two distinct regions with different slopes. Below 250 μm, the slopes are 1.67-1.92, while they are much steeper above 250 μm with slopes 5.5-6.The depth-averaged PSD for ES1 (over all depths) is shown in Figure 5i. While multiple segmented slopes have been observed in prior oceanic data,[7,20] a recent study postulates turbulence could be the primary driver in this segmented slope, potentially correlated to particle aggregation/breaking.[21] The authors tie particle breakage/aggregation and relate it to local turbulence structure, specifically the Kolmogorov length scale $\eta = (\frac{\nu^3}{\epsilon})^{1/4}$. Here, ν is the

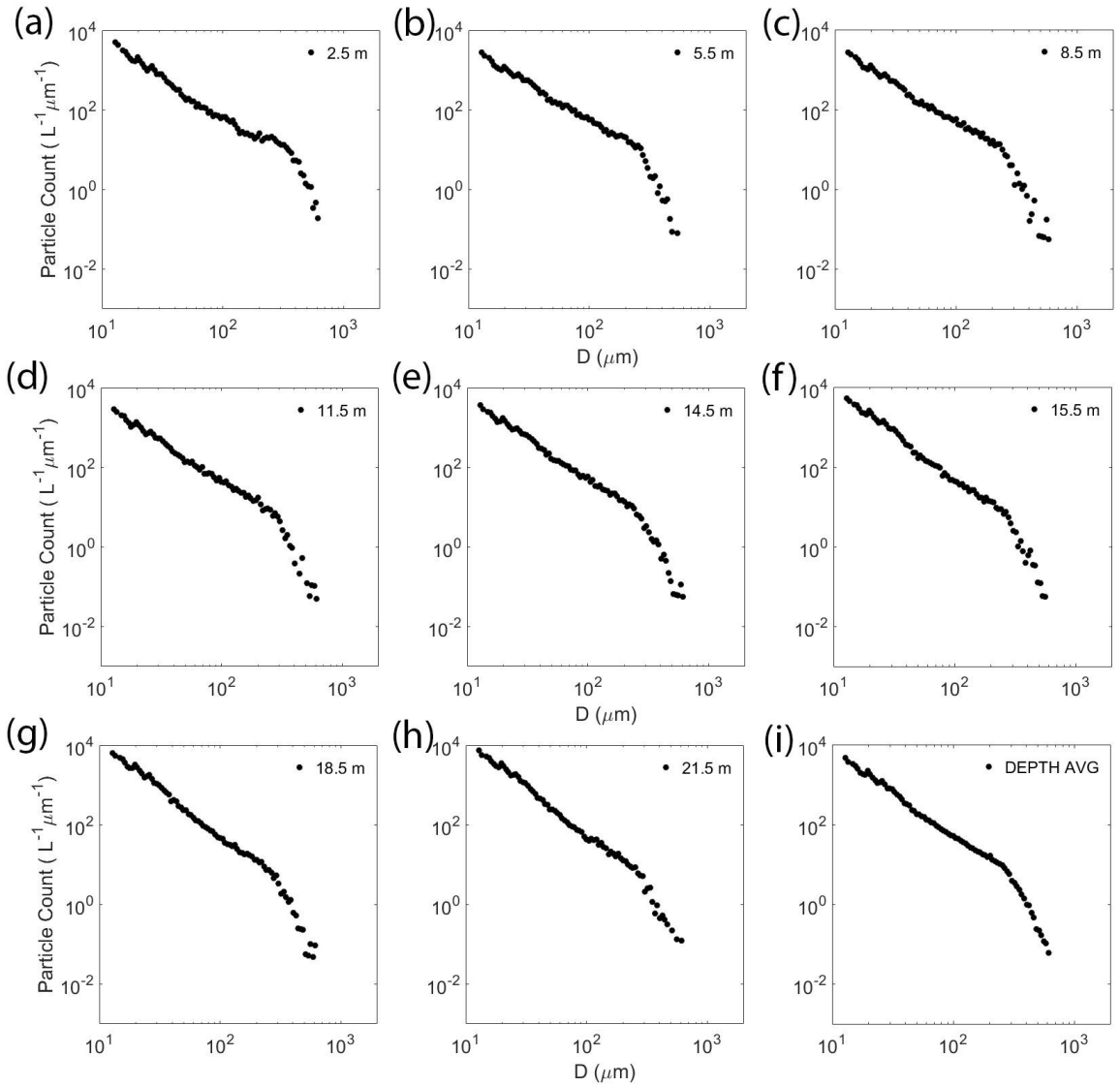

Figure 5. PSDs at 3 m depth bins for ES1: (a) 2.5 m; (b) 5.5 m; (c) 8.5 m; (d) 11.5 m; (e) 14.5 m; (f) 17.5 m; (g) 20.5 m; and (h) 23.5 m. (i) Depth averaged PSD over entire water column.

kinematic viscosity of seawater (1.1 x $10^{-6} m^2 s^{-1}$), and ϵ is the turbulent kinetic energy (TKE) dissipation rate. In our case, the ADV data can be used to estimate the local TKE dissipation rate, and consequently η, which lies between 1.2-1.5 mm for this station. This value is several times larger than the value of D where the slope changes (300 μm), leading to the conclusion that D is not the correct length scale, at least in our data. The MAL could be a more appropriate length scale for this analysis, and we will look to explore this in the future. While our limited data prohibits an exhaustive study, a qualitative approach might hint at the effect turbulence plays in breaking particles. During the depth profiles for ES1 and ES2, data is recorded during both downcasts and upcasts. As mentioned before, downcasts are relatively slow and gently done so as to ensure minimum disturbance to the particle field. On the other hand, the sampling volume is in the wake of the system during upcasts, thus leading to a highly turbulent flow in this region. In Figure 6, the particles are first binned into several aspect ratio groups and then a percentage change in particle populations within each bin is calculated. A positive value indicates that more number of particles in a particular aspect ratio bin were present during

the upcast rather than the downcast, while a negative value indicates the opposite. At both stations, it can be seen that there are a greater number of small aspect ratio particles during the upcast and greater number of large aspect ratio particles during the downcast. This pattern is consistent with the expectation that higher turbulence leads to particle breakage, and thus lead to higher number of small particles in a given population.

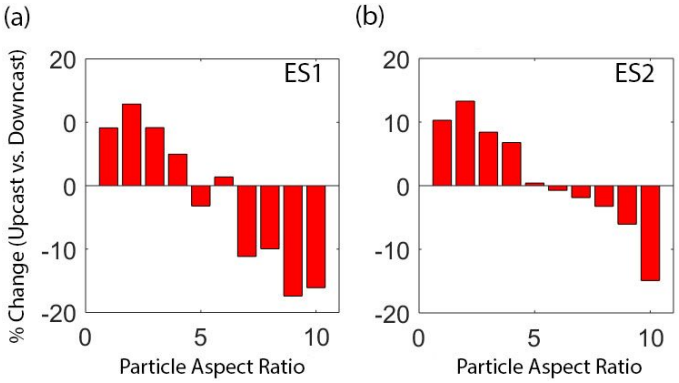

Figure 6. Percentage change in the number of particles during downcast and upcast in any given aspect ratio bin for (a) ES1; and (b) ES2.

3.2 Lake Erie, Michigan

Lake Erie, one of the five Great Lakes, is a large freshwater body at the US-Canadian border. There has been an increasing occurrence of harmful algal blooms (HABs) here in the last couple of decades, characterized by the enhanced presence of certain cyanobacterial species. In western Lake Erie, which is the focus of this particular analysis, summer blooms are particularly driven by the cyanobacteria belonging to *Microcystis sp.* The increasing HAB formations have been attributed to various factors such as climate change, eutrophication of waters due to increasing nutrient runoffs from surrounding areas, and/or introduction of alien species which potentially upset the ecosystem balance.[22] These HABs can render water unfit for consumption, affect human health and recreational activities. Thus, understanding the properties of HABs and the underlying mechanisms that drive them is essential. To this end, a large, inter-institutional collaborative effort to study the bio-optical properties of the cyanobacterial HABs was carried out in Western Lake Erie in August 2014.[23] Different instrumentation included sensors to measure the inherent optical properties (IOPs) through either vertical profiles or in towed mode, as well as remote sensing reflectance. A detailed analysis of the data and other related conclusions can be found elsewhere.[23] The HOLOCAM was deployed separately (but in close vicinity to the other packages), with the goal of characterizing the particle fields, with a special focus on *Microcystis* colony size and structure in the water column. Two datasets taken in quick succession on August 21, 2014 (denoted as LE1 and LE2), in an area dominated by *Microcystis* will be discussed here. For LE1, 795 holograms were included as part of the analysis, while the corresponding number for LE2 was 850. A sample raw hologram with a Microcystis colony is shown in Figure 7.

3.2.1 Particle size distributions

The PSD analysis methodology here remains the same as in the East Sound data discussed in section 3.1. The PSD variations with depth for LE1 and LE2, along with the depth-averaged PSD are presented in Figures 8a and 8b. For both these cases, the data has been binned at 1 m depths, and centered around 1 m, 2 m etc. Only the topmost bin is narrower, with a 0.5 m depth and centered at 0.25 m. The PSD is characterized by a lack of two distinct linear segments as seen in the East Sound particle fields. There is only one linear region between 50-150 μm, where the slope is about -2.5 for both stations. However, a distinct bump is seen at D = 300 μm in the top three bins at both stations, especially noticeable for LE1. This bump represents an enhanced presence of particles at or around that equivalent size diameter range. This interesting phenomenon was missing at other stations in Lake Erie where *Microcystis* was absent or present in low numbers.[23] Previous studies[23] also link this size range to impact of colony size on vertical migration - for example, maximum ranges of migration occurred when

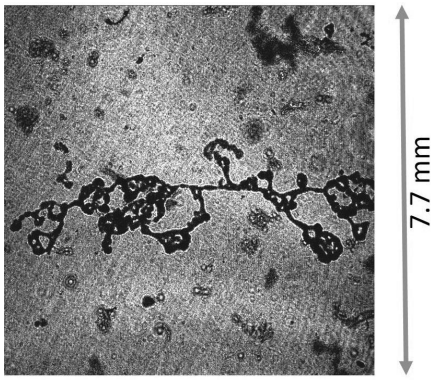

Figure 7. Sample raw hologram (without image corrections) showing a *Microcystis* colony. To provide a measure of the colony size, the cropped field of view is 7.7 x 7.7 mm here.

colonies were 200 μm in size.[24] Thus, it is important to isolate the *Microcystis* colonies from the other particles to study this aspect further. Figures 8c and 8d show the histogram of the *Microcystis* colony sizes (after segregating them from the general particle population) for both stations. As the figures clearly depict, most of the colonies in the resolved size ranges are clustered around 200-300 μm, again coinciding with the optimal size for vertical migration. Our data also provides the ability to estimate the cell counts of *Microcystis*, based on colony size. Juong et al.[25] carried out a controlled study and conclude that the the cell counts correlate more closely with the volume of a given colony, rather than the colony area. They propose the following empirical relationship: C = 0.00195V + 1931, where C is the number of cells and V is the volume of any given colony. Based on the isolated colonies from the holographic data, we can use the above relationship and get an estimate of the vertical structure of the cell counts in the water column. It should be noted that this analysis is based on only large aggregates which can be definitely isolated and identified as *Microcystis* colonies, and ignores smaller colonies and/or individual cells. While this approach leads to lower error in other particles being wrongly identified as *Microcystis*, it also very likely underestimates the actual cell counts. Figures 9a and 9b show the vertical profiles for the cell counts, binned at 0.5 m depths. Both show similar trends, with a high concentration of *Microcystis* cells in the topmost bin (1.35 x 10^6 cells/mL). The concentration drops uniformly with depth upto 4.25-4.5 m, where it is only a quarter of the surface cell count. Below this, however, the cell counts pick up over the bottom 1-2 m, almost reaching 1 x 10^6 cells/mL at the bottom-most sampled location.

3.3 Gulf of Mexico

As part of a cruise of opportunity, the HOLOCAM was deployed in the Gulf of Mexico in May 2017, together with certain ancillary instrumentation (optical and acoustic sensors). The areas sampled included the Mississippi river outflow into the Gulf, which is laden with a rich variety of particles, ranging from organic detrital matter to sediments to diverse phyto/zooplankton. Several profiles were also acquired in relatively clear waters in the deep waters of the Mississippi Canyon, representative of the open ocean. In total, 60 different stations were sampled, leading to acquisition of several TB of holographic images.

3.3.1 Current work

Work is currently underway to tackle the large database in a structured manner. Figure 10 provides an illustration of a typical depth profile and the variety of organisms present at different regions in the stratified water column, along with the vertical density (σ_T) structure. The primary goal with this holographic database is to create training sets using several thousand in-focus images of various species. Automated classifiers would then potentially be able to segregate particles into various groups,[26] thus facilitating studies on various scientific questions including quantification of nearest neighbor distances, spatial patterns between various phytoplankton/zooplankton which could provide insights into predator-prey interactions, etc. While several *in situ* studies in these areas have been carried out, the results have been limited by existing technology at those times.[27,28] Re-approaching these questions and tackling them using current data analysis techniques could open up hitherto unexplored avenues of research.

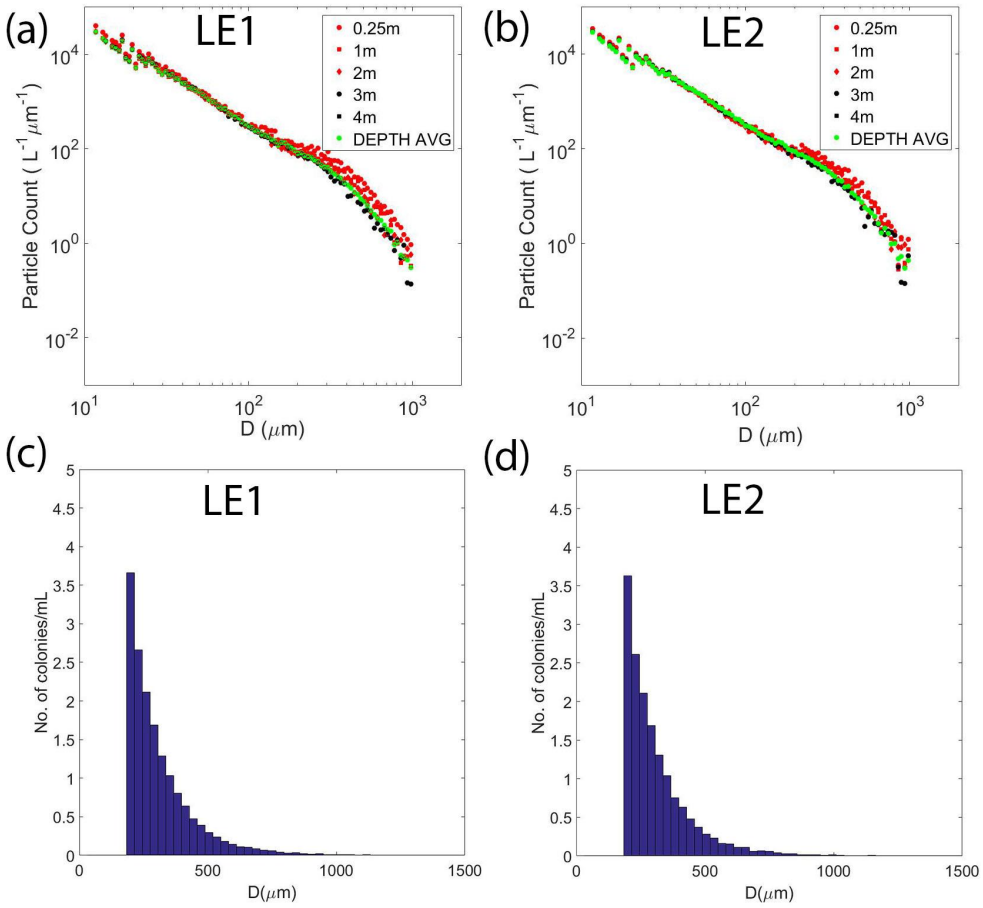

Figure 8. PSD variations with depth for (a)LE1; and (b) LE2, with the depth-averaged PSD overlaid. Histograms of colony concentrations in various size ranges for (c) LE1; and (d) LE2.

4. SUMMARY AND DISCUSSION

Several field deployments of a digital submersible holographic imaging system (HOLOCAM) in diverse aquatic environments have been detailed. The inherent advantage of holography over standard 2-D imaging is the ability to sample remote, undisturbed volumes, and characterize *in situ* particle fields at high resolutions. Particles quantified include marine detrital matter and different planktonic species. At East Sound, the presence of a 'thin layer' of enhanced particle abundance was recorded, coinciding with a strong pycnocline. The 'thin layer' was dominated by *Ditylum brightwellii*, a species of colonial diatom. Vertical distributions show that while the diatom chains across the resolved length ranges were present uniformly at higher concentrations within the layer, almost all of the longest chains were concentrated within the layer itself. The difference in aspect ratios of particles during downcasts and upcasts also shed some qualitative insight into the effect of turbulence in breaking of particles. At Lake Erie, the presence of a HAB, driven by enhanced concentrations of the cyanobacterial species *Microcystis*, was reported. The PSDs for the entire particle field show a distinct bump in the size range where enhanced migration of *Microcystis* colonies have been reported. This trend is supported by the histogram of various sizes of isolated *Microcystis* colonies which show that most colonies are in the 250-300 μm size range. Finally, the rich diversity of planktonic species and a successful data collection cruise in the Gulf of Mexico have been discussed. The vast database of holographic data will act as an ideal training set to implement machine learning algorithms for facilitation of particle segregation into different groups. If successful, this would be a significant step towards facilitating studies on *in situ* biophysical interactions, including but not limited to, 3-D spatial patterns, predator-prey interactions, and heterogeneity in plankton communities in the ocean.

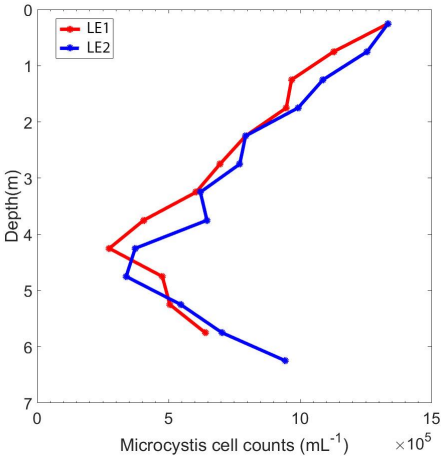

Figure 9. Vertical profiles of *Microcystis* cell counts using the empirical relationship provided in Juong et al.[25] for (a) LE1; and (b) LE2.

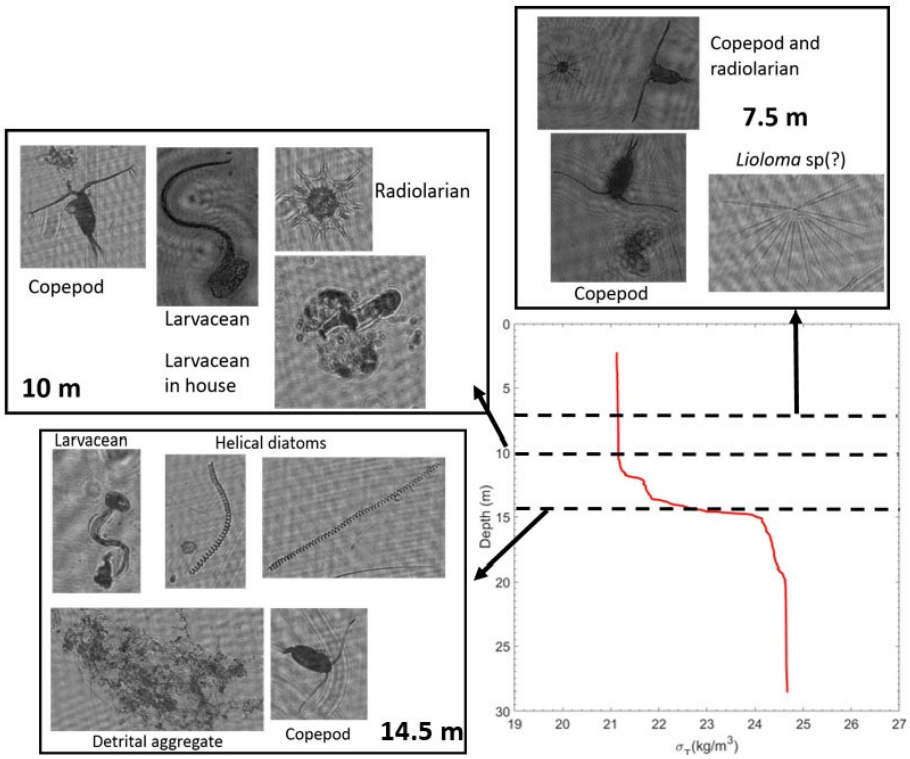

Figure 10. Collage of different planktonic species at various depths during a single vertical profile in coastal Gulf of Mexico waters, illustrating the rich diversity.

ACKNOWLEDGMENTS

The authors would like to thank Tim Moore, Jeffrey Krause and Alan Weidemann for providing invaluable support to obtain field data on cruises of opportunity, and Nicole Stockley for help with data acquisition. The authors also gratefully acknowledge funding provided for this work from the Office of Naval Research Coastal and Geophysics Program, National Science Foundation (NSF) Ocean Technology and Interdisciplinary Coordination Program (OCE-1634053), NSF Biological Oceanography (OCE-1657332), NOAA CIOERT, Harbor Branch Oceanographic Institute Foundation and the HBOI Specialty License Plate program.

REFERENCES

[1] Lal, D., "The oceanic microcosm of particles," *Science* **198**, 997–1009 (1977).

[2] Honjo, S., Eglinton, T., Taylor, C., Ulmer, K., S.Sievert, A.Bracher, German, C., Edgcomb, V., Francois, R., and Inglesias-Rodriguez, M., "Understanding the role of the biological pump in teh global carbon cycle: An imperative for ocean science," *Oceanography* **27(3)**, 10–16 (2014).

[3] Hsu, T., Traykovski, P., and Kineke, G., "On modeling boundary layer and gravity-driven fluid mud transport," *J.Geophys.Res* **112(C4)**, C04011 (2007).

[4] Hackett, E., L.Luznik, A.R.Nayak, J.Katz, and Osborn, T., "Field measurements of turbulence at an unstable interface between current and wave boundary layers," *J.Geophys.Res* **116(C2)**, C02022 (2011).

[5] Nayak, A., Li, C., Kiani, B., and Katz, J., "On the wave and current interaction with a rippled seabed in the coastal bottom boundary layer," *J. Geophys. Res.* **120(7)**, 4595–4624 (2015).

[6] Marcos, Seymour, J., Luhar, M., Durham, W., Mitchell, J., Macke, A., and Stocker, R., "Microbial alignment in flow changes ocean light climate," *Proc. Nat. Acad. Sci.* **108**, 3860–3864 (2011).

[7] Nayak, A., McFarland, M. N., Sullivan, J. M., and M.S.Twardowski, "Evidence for ubiquitous preferential particle orientation in representative oceanic shear flows," *Limnol. Oceanogr.* **21**, 1087–1091 (2018).

[8] Holliday, D., Donaghay, P., Greenlaw, C., Napp, J., and Sullivan, J., "High frequency acoustics and bio-optics in ecosystems research," *ICES J. Mar. Sci.* **66(6)**, 974–980 (2009).

[9] McManus, M., Alldredge, A., Barnard, A., Boss, E., Case, J., Cowles, T., Donaghay, P., Eisner, L., Gifford, D., and Greenlaw., C., "Characteristics, distribution and persistence of thin layers over a 48 hour period," *Mar. Ecol. Prog. Ser.* **261**, 1–19 (2003).

[10] Jaffe, J., "Underwater optical imaging: The past, the present, and the prospects.," *IEEE J. Oceanic Engg.* **40(3)**, 683–700 (2015).

[11] Talapatra, S., Sullivan, J., Katz, J., M.Twardowski, H.Czerski, P.Donaghay, Hong, J., Rines, J., M.McFarland, A.R.Nayak, and C.Zhang, "Application of in situ digital holography in the study of particles, organisms and bubbles within their natural environment," in [*Ocean Sensing and Monitoring IV*], *Proc. SPIE* **8372**, 837205 (2012).

[12] Talapatra, S., Hong, J., McFarland, M., Nayak, A., Zhang, C., Katz, J., Sullivan, J., Twardowski, M., Rines, J., and Donaghay, P., "Characterization of biophysical inteactions in the water column using in situ digital holography," *Mar. Ecol. Prog. Ser.* **473**, 29–51 (2013).

[13] Schnars, U. and Jueptner, W., [*Digital holography*], Springer, Berlin Heidelburg (2005 (first edition)).

[14] Katz, J. and Sheng, J., "Applications of holography in fluid mechanics and particle dynamics," *Annu. Rev. Flu. Mech.* **42**, 531–555 (2010).

[15] McFarland, M., Rines, J., Sullivan, J., and Donaghay, P., "Impact of phytoplankton size and physiology on particulate optical properties determined with scanning flow cytometry," *Mar. Ecol. Prog. Ser.* **531**, 43–61 (2015).

[16] Twardowski, M., Sullivan, J., and Dalgleish, F., "Study undisturbed particle fields in the ocean: Novel instrument suite for more representative particle measurements," *Sea Tech.* **57(2)**, 15–17 (2016).

[17] Durham, W. and Stocker, R., "Thin phytoplankton layers: characteristics, mechanisms, and consequences," *Annu. Rev. Mar. Sci.* **4**, 177–207 (2012).

[18] Kitchen, J., Zaneveldan, J., and Pak, H., "Effect of particle size distribution and chlorophyll content on beam attenuation spectra," *Appl. Opt.* **21**, 3913–3918 (1982).

[19] Twardowski, M., Boss, E., MacDonald, J., Pegau, W., Barnard, A., and Zaneveld, J., "A model for estimating bulk refractive index from optical backscattering ratio and the implications for understanding particle composition in case i and case ii waters," *J. Geophys. Res.* **106**, 14129–14142 (2001).

[20] Sullivan, J., Twardowski, M., Donaghay, P., and Freeman, S., "Use of optical scattering to discriminate particle types in coastal waters," *Appl. Opt.* **44**, 1667–1680 (2005).

[21] Takeuchi, M., Doubell, M., Jackson, G., Mitchell, J., and Yamazaki, H., "Turbulence controls size distribution of aggregates: in situ observations by a microstructure profiler," in [*AGU/ASLO/TOS Ocean Sciences Meeting, Protland, Oregon, February 11-16,*], (2018).

[22] Paerl, H., Hal, N., and Calandrino, E., "Controlling harmful cyanobacterial blooms in a world experiencing anthropogenic and climatic-induced change," *Sci. Total Environ.* **409**, 1739–1745 (2011).

[23] Moore, T., Mouw, C., Sullivan, J., M.Twardowski, Burtner, A., Ciochetto, A., McFarland, M., Nayak, A., Paladino, D., Stockley, N., Johengen, T., Yu, A., Ruberg, S., and Weidemann, A., "Bio-optical properties of cyanobacterial blooms in western lake erie," *Front. Mar. Sci.* **4**, 300 (2017).

[24] Visser, P., Passarge, J., and Mur, L., "Modelling vertical migration of the cyanobacterium microcystis," *Hydrobiologia* **349**, 99–109 (1997).

[25] Juong, S.-H., Kim, C.-J., Ahn, C.-Y., Jang, K.-Y., Boo, S., and Oh, H.-M., "Simple method for a cell count of the colonial cyanobacterium, microcystis sp.," *Kor. J. Microbio.* **44(5)**, 562–565 (2006).

[26] Sosik, H. and Olson, R., "Automated taxonomic classification of phytoplankton sampled with imaging-in-flow cytometry," *Limn. Oceanogr.: Methods* **5(6)**, 204–216 (2007).

[27] Malkiel, E., Alquaddoomi, O., and Katz, J., "Measurements of plankton distribution in the ocean using submersible holography," *Meas. Sci. Tech.* **10**, 1142 (1999).

[28] Malkiel, E., Abras, J., Widder, E., and Katz, J., "On the spatial distribution and nearest neighbor distance between particles in the water column determined from in situ holographic measurements," *J. Plank. Res.* **28(2)**, 149–170 (2006).